The first University in Korea Soongsil University

Neutrino Reactions on nuclei of astrophysical importance by QRPA and Deformed QRPA

Myung-Ki Cheoun

Soongsil University, Seoul, Korea

K. S. Kim, E. Ha, C. Ryu, K. Choi, Y. Kwon, T. Miyatsu..
G. Mathews , A. Brown..
T. Kajino, K. Nakamura, T. Hayakawa, S. Chiba,
T. Maruyama …

The 1st Visiting NAOJ Fellow Workshop
-Element Genesis and Cosmos Chemical Evolution r-process perspective-
- RIKEN, Nishina Hall, Wako, Japan, Oct. 13-15

Contents

Motivation in theoretical description

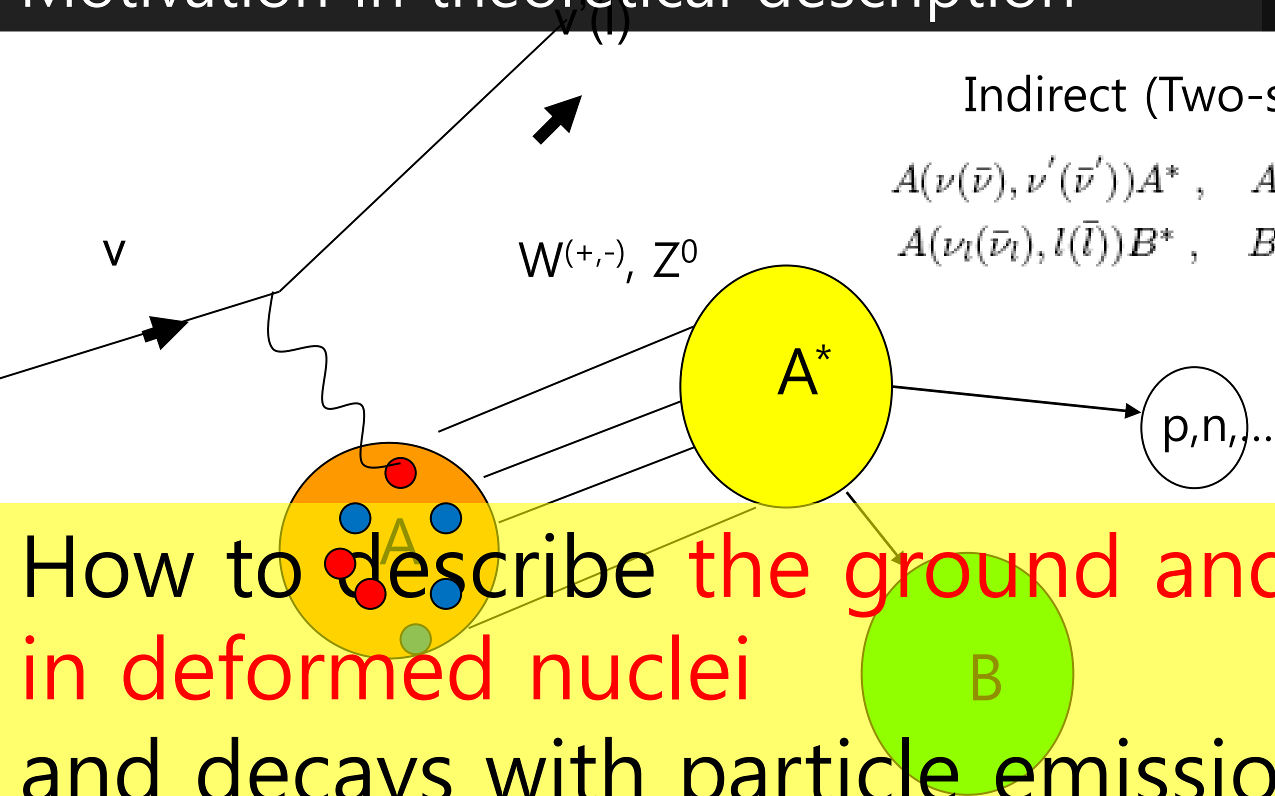

Indirect (Two-step) Processes

$$A(\nu(\bar{\nu}),\nu'(\bar{\nu}'))A^* \ , \quad A^* \rightarrow B + \text{outgoing particles.}$$
$$A(\nu_l(\bar{\nu}_l),l(\bar{l}))B^* \ , \quad B^* \rightarrow C + \text{outgoing particles}$$

How to describe the ground and excited states in deformed nuclei and decays with particle emissions ?

by using Hauser-Feshbach statistical model by S.Chiba

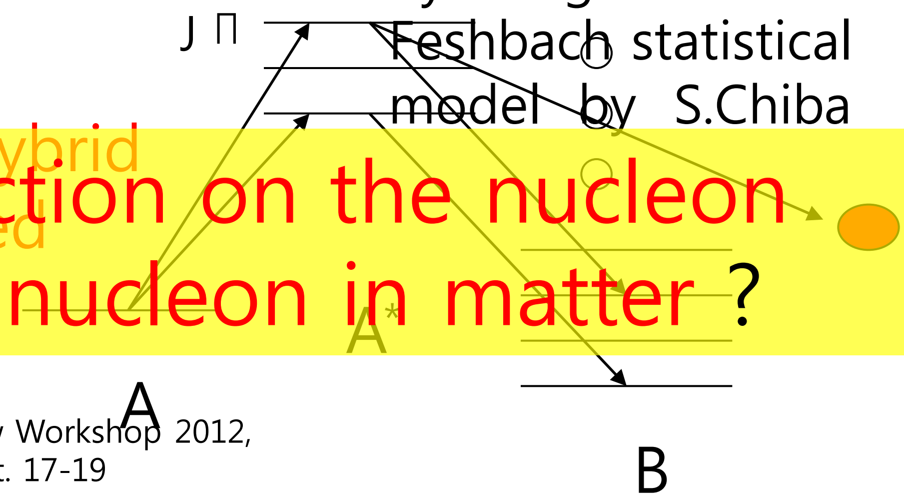

SM, QRPA, Hybrid And Deformed QRPA

How to describe the reaction on the nucleon bound in nuclei and the nucleon in matter ?

Various roles of ν's in SN-nucleosynthesis

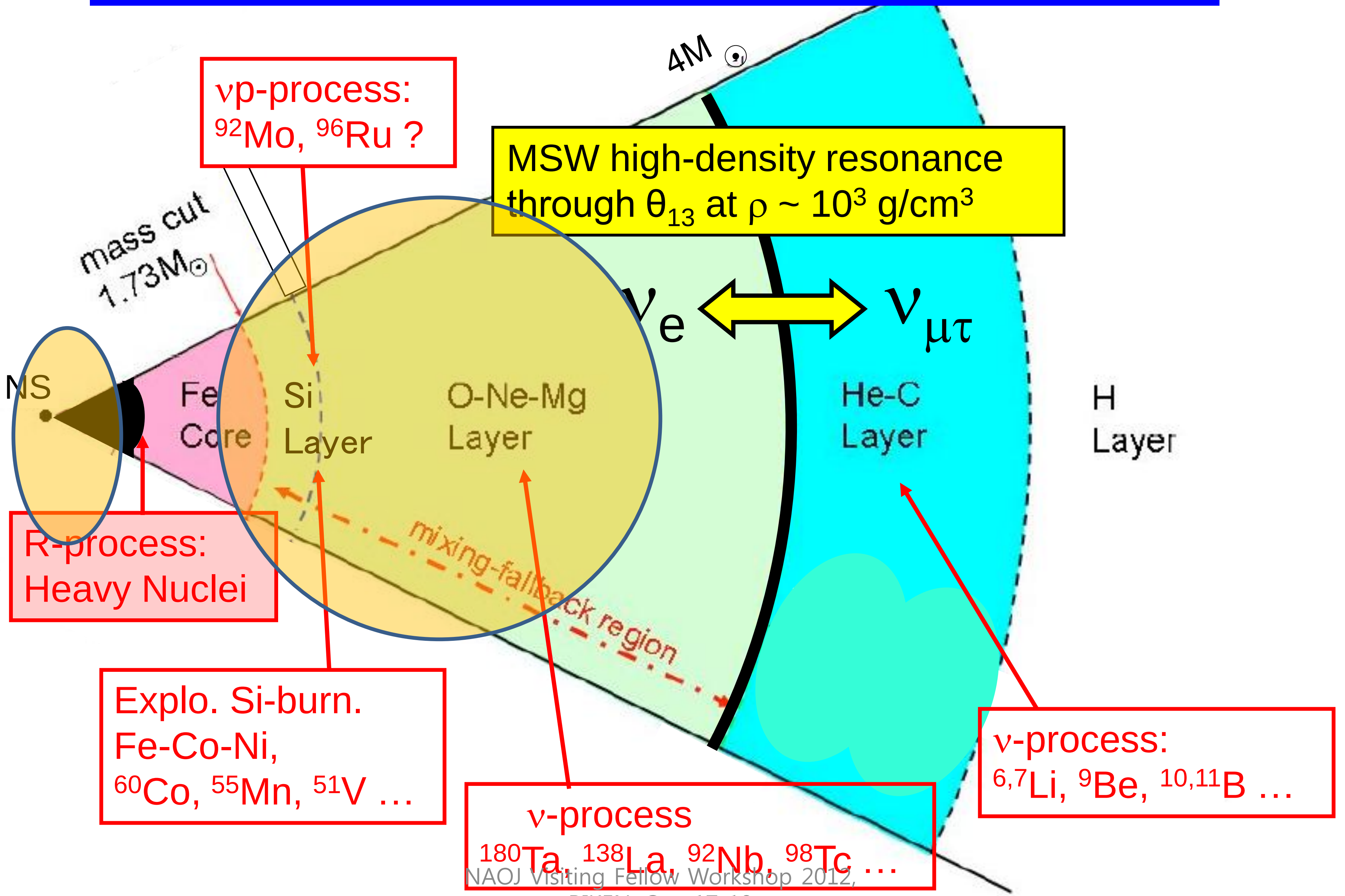

From Toshitaka Kajino

Octet baryon electromagnetic form factors in nuclear medium

G. Ramalho[1], K. Tsushima[2], and A. W. Thomas[2,3]

[1] *CFTP, Instituto Superior Técnico, Univesidade Técnica de Lisboa, Av. Rovisco Pais, 1049-001 Lisboa, Portugal*
[2] *CSSM and* [3] *CoEPP, School of Chemistry and Physics, University of Adelaide, Adelaide SA 5005, Australia*

(Dated: June 12, 2012)

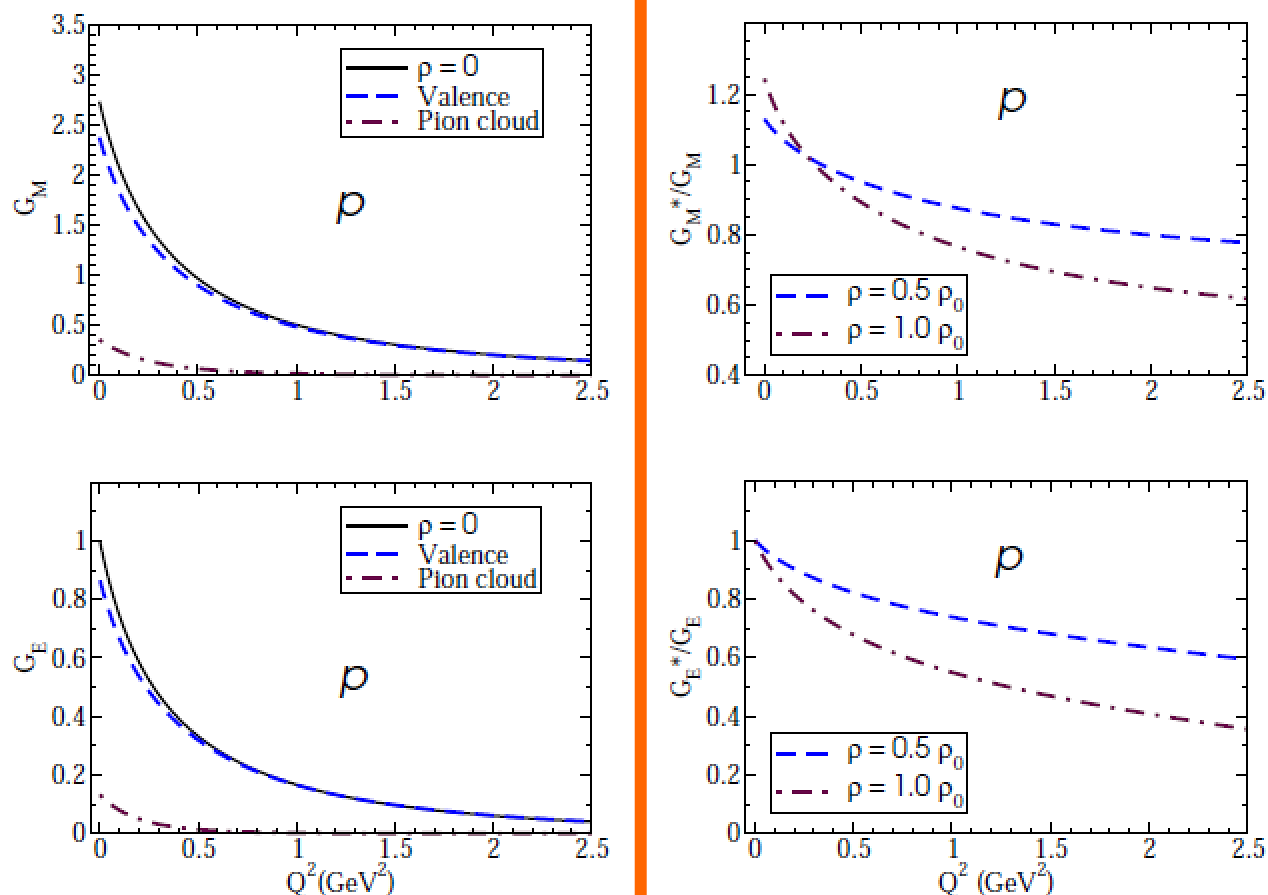

FIG. 4: Proton electromagnetic form factors calculated for $\rho = 0$ (vacuum) with a decomposition of the valence and pion cloud contributions (left panel), and the ratios to those of the $\rho = 0$ (right panel) for $\rho = 0.5\,\rho_0$ (dashed line) and $1.0\,\rho_0$ (dash-doted line).

2.1. Relativistic mean field Lagrangian

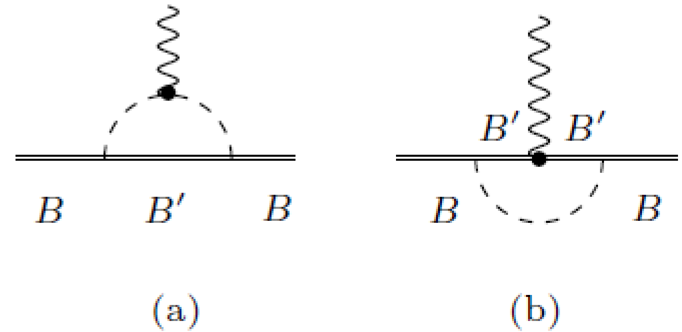

FIG. 1: Electromagnetic interaction with the baryon B within the one-pion loop level through the intermediate baryon states B'. A diagram including a contact vertex $\gamma\pi BB'$, as described in Ref. [20], is not represented explicitly, since the isospin structure is the same as diagram (a). See Ref. [20] for details.

$$
\begin{aligned}
\mathscr{L} = & \sum_b \bar{\psi}_b \Big[i\gamma_\mu \partial^\mu - q_b \gamma_\mu A^\mu - M_b^*(\sigma, \sigma^*) - g_{\omega b}\gamma_\mu \omega^\mu - g_{\phi b}\gamma_\mu \phi^\mu \\
& - g_{\rho b}\gamma_\mu \vec{\tau} \cdot \rho^\mu - \frac{1}{2}\kappa_b \sigma_{\mu\nu} F^{\mu\nu} \Big] \psi_b + \sum_l \bar{\psi}_l \left[i\gamma_\mu \partial^\mu - q_l \gamma_\mu A^\mu - m_l \right] \psi_l \\
& + \frac{1}{2}\partial_\mu \sigma \partial^\mu \sigma - \frac{1}{2} m_\sigma^2 \sigma^2 - U(\sigma) + \frac{1}{2}\partial_\mu \sigma^* \partial^\mu \sigma^* - \frac{1}{2} m_{\sigma^*}^2 \sigma^{*2} \\
& - \frac{1}{4} W_{\mu\nu} W^{\mu\nu} + \frac{1}{2} m_\omega^2 w_\mu w^\mu - \frac{1}{4}\Phi_{\mu\nu}\Phi^{\mu\nu} + \frac{1}{2} m_\phi^2 \phi_\mu \phi^\mu \\
& - \frac{1}{4} R_{i\mu\nu} R_i^{\mu\nu} + \frac{1}{2} m_\rho^2 \rho_\mu \rho^\mu - \frac{1}{4} F_{\mu\nu} F^{\mu\nu},
\end{aligned}
\tag{1}
$$

Effective Mass in nuclear medium

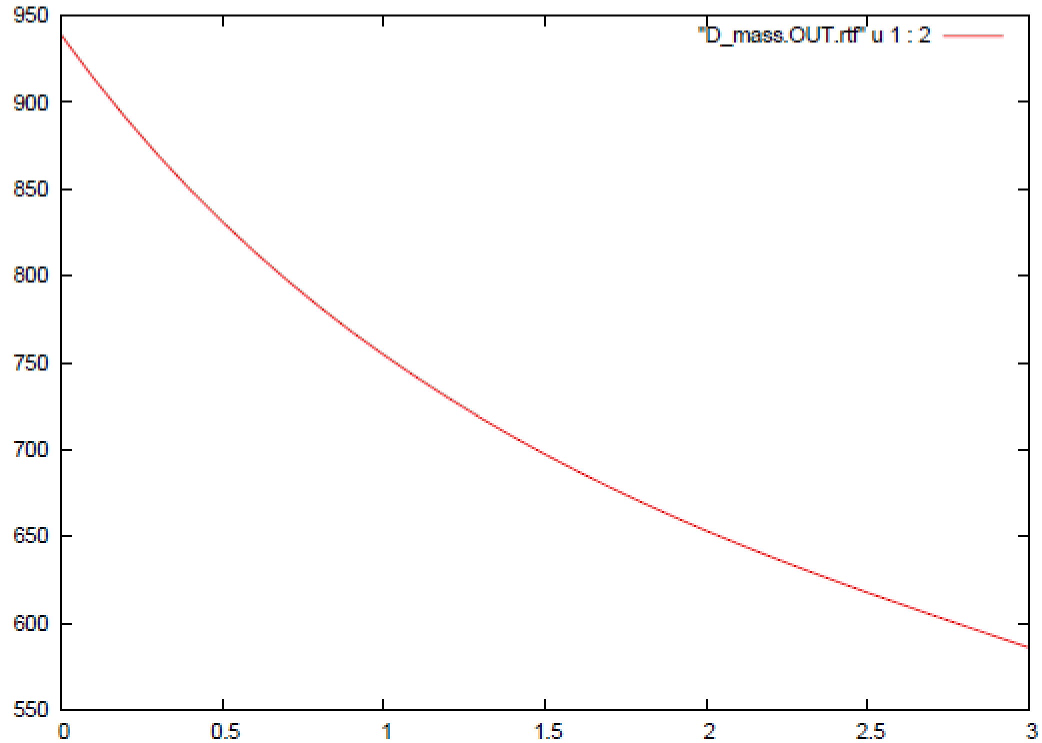

FIG. 4: The effective mass $M^*(\rho)$ in terms of finite density ρ/ρ_0.

[QMC(medium)]/[QMC(vacuum)] for g_A.

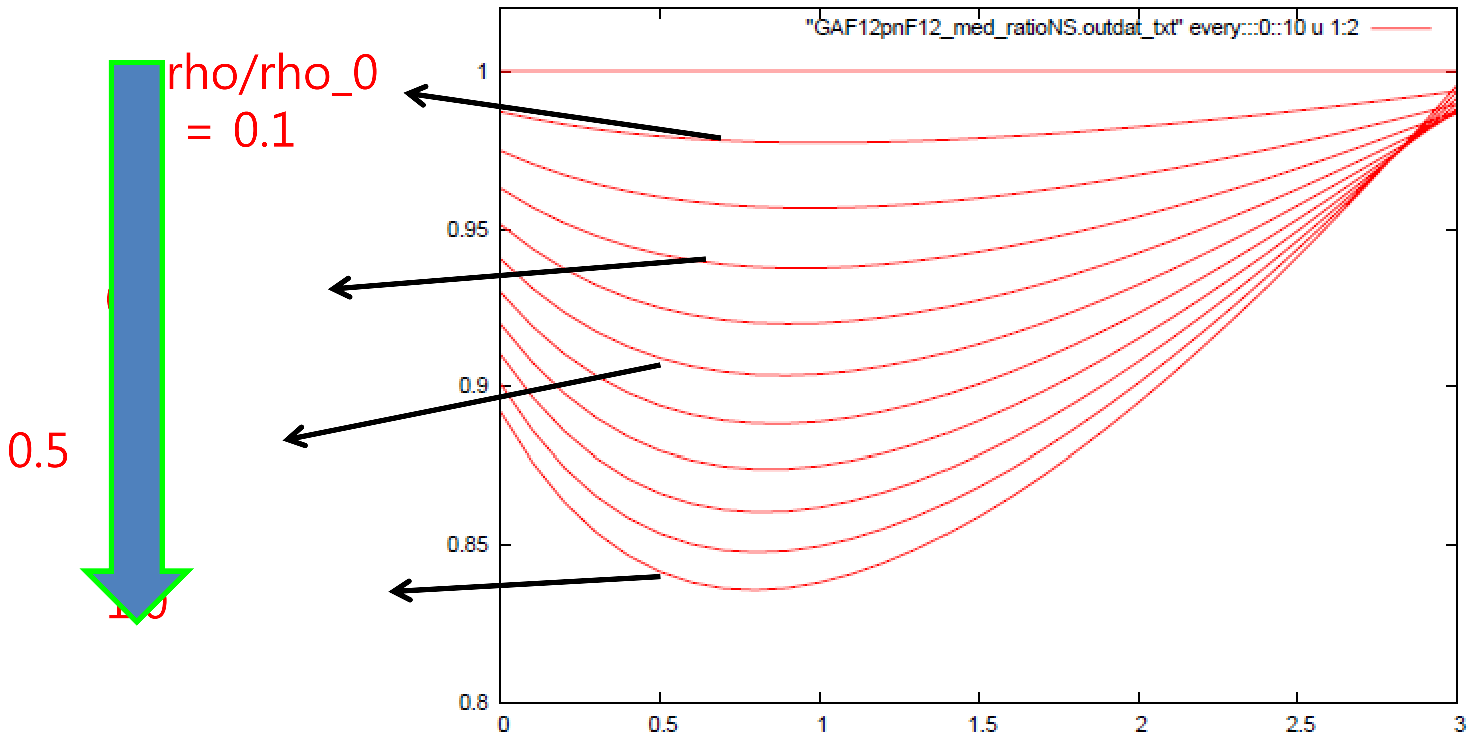

FIG. 1: Change of the axial coupling constant normalized to that in free space, $g_A(\rho, Q^2)/g_A(\rho = 0, Q^2)$, with finite momentum transfer in nuclear medium. From the uppermost (vacuum), density ratios are increased by 0.1 ρ_0. Lowermost curve is for $\rho = \rho_0$.

[QMC(medium)]/[QMC(vacuum)] for F1.

$$F_1^V(Q^2) = F_{1p}(Q^2) - F_{1n}(Q^2),$$
$$F_2^V(Q^2) = F_{2p}(Q^2) - F_{2n}(Q^2).$$

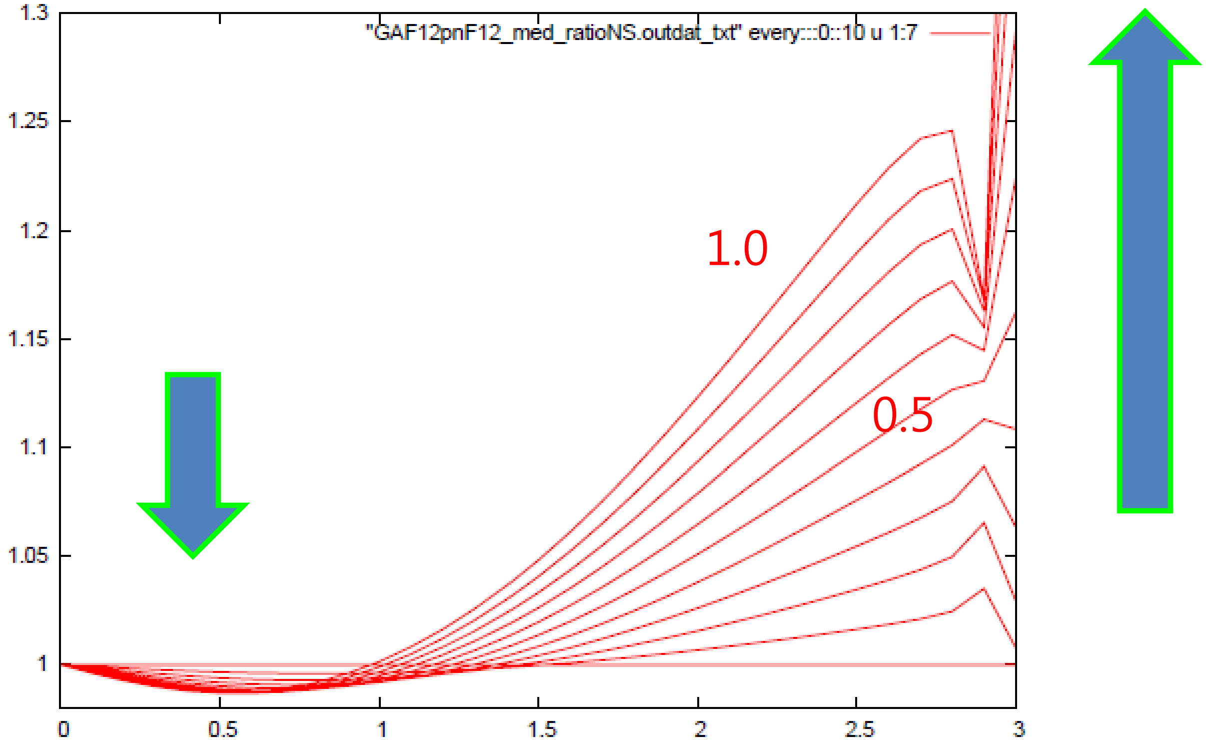

FIG. 2: Change of the weak coupling constant ratio, $F_1(\rho, Q^2)/F_1(\rho = 0, Q^2)$, with finite momentum transfer in nuclear medium. From the lowermost (vacuum), density ratios are increased by 0.1 ρ_0. Uppermost curve is for $\rho = \rho_0$.

[QMC(medium)]/[QMC(vacuum)] for F2.

$$F_1^V(Q^2) = F_{1p}(Q^2) - F_{1n}(Q^2),$$
$$F_2^V(Q^2) = F_{2p}(Q^2) - F_{2n}(Q^2).$$

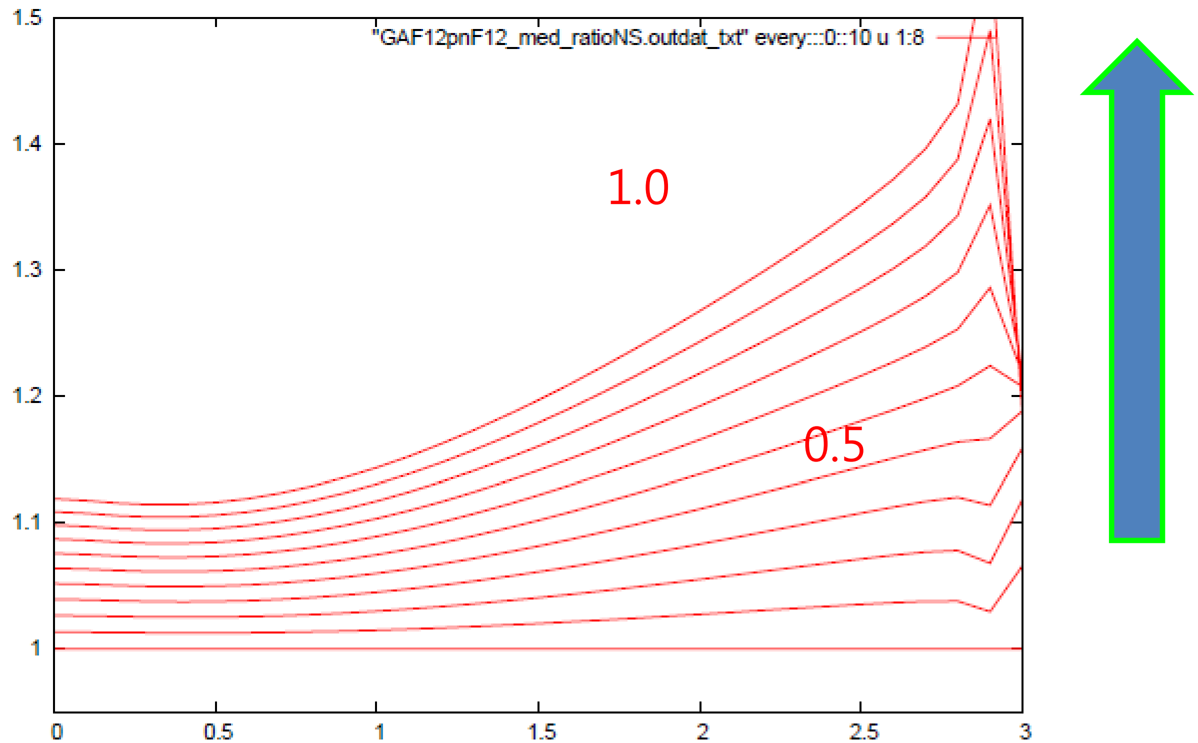

FIG. 3: Changed of the weak coupling constant ratio, $F_2(\rho, Q^2)/F_2(\rho = 0, Q^2)$, with finite momentum transfer in nuclear medium. From the lowermost (vacuum), density ratios are increased by 0.1 ρ_0. Uppermost curve is for $\rho = \rho_0$.

Neutrino X-section on the nucleon in dense matter

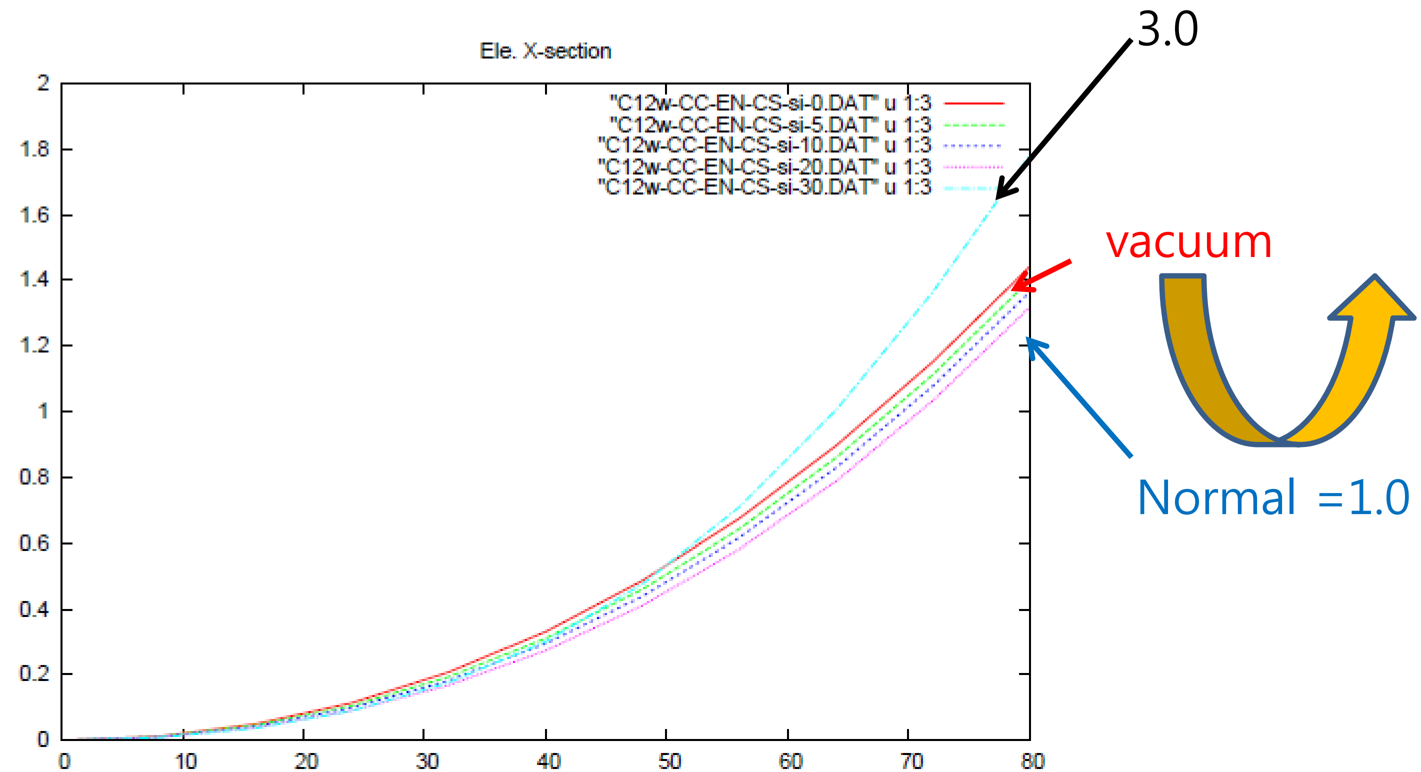

FIG. 5: Density dependence of electro-neutrino cross sections on a proton. The y axis is $10^{-41} cm^2$ and x-axis is the incident neutrino energy in the units of MeV. Red curve is the result in free space. The cross sections are decreased with the increase of the density by 0.1 ρ/ρ_0, but it is increased suddenly at 3 ρ_0.

About 10 (normal) - 40 %(3 rho_0) decrease of the cross sections on a proton !!

Density dependence of X-section on 12C via CC

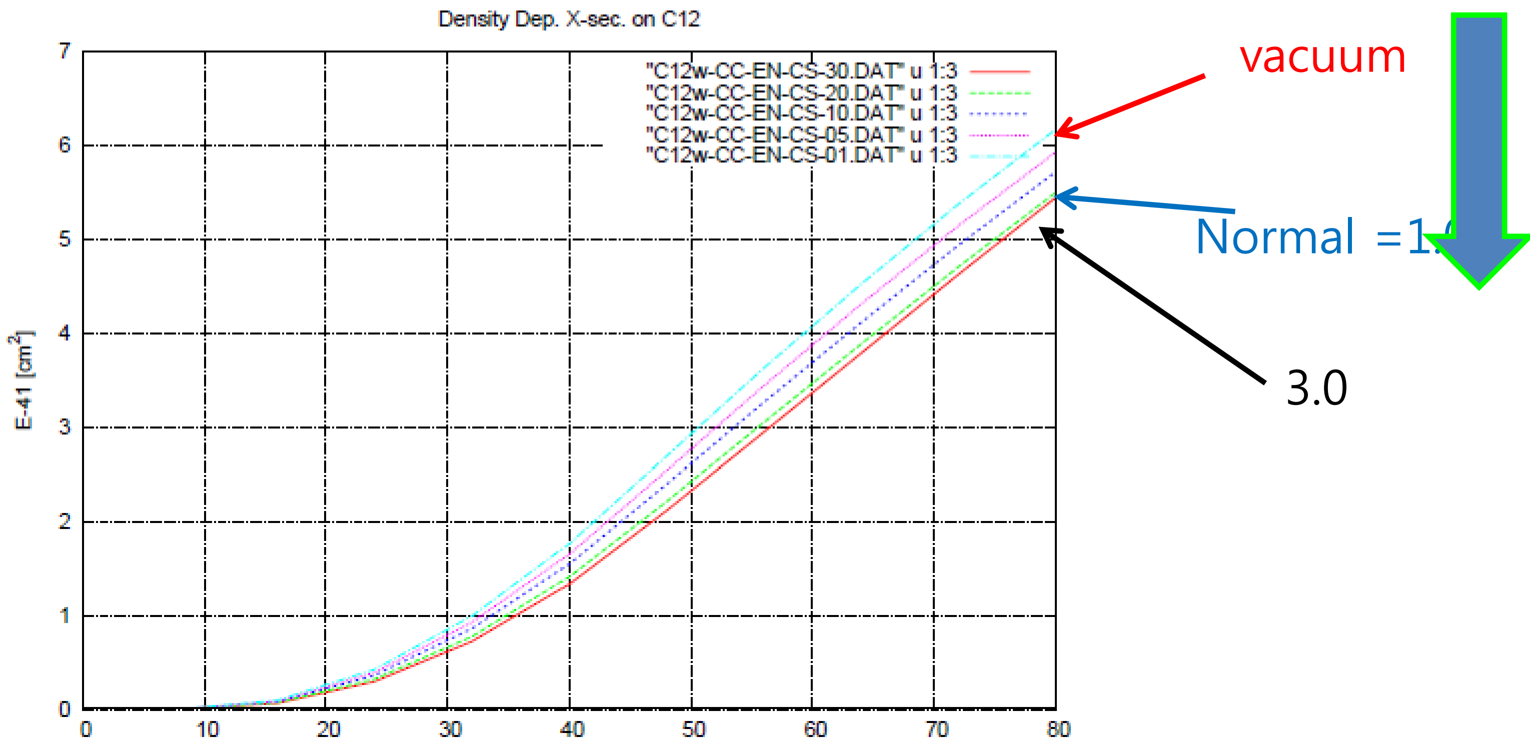

FIG. 6: Density dependence of electro-neutrino cross sections on ^{12}C. The y axis is $10^{-41} cm^2$ and x-axis is the incident neutrino energy in the units of MeV. The cross sections are decreased with the increase of the density by 0.1 ρ/ρ_0.

About 10 (normal) - 15 %(3 rho_0) decrease of the cross section s for 12 C !!

Contents

1. Motivation
1-1. Supernovae Neutrinos and Nu-p and Nu-process in SNe
1-3. Cosmological origins of P-nuclei

2. Theoretical Description of Neutrino induced reaction
2-1. Lessons from 12C reaction data
2-2. Neutrino reactions on bound nucleons in nucleus and nucleons in nuclear matter
2-3. High-lying GT states in Neutrino Reaction

3. Applications to Neutrino Reactions
3-1. GT strengths and Neutrino reactions for ^{90,92}Nb and ^{40}Ar by QRPA
3-2. GT strengths and Neutrino reactions for $^{26-34}$Mg, ^{82}Se, ^{76}Ge by DQRPA

4. Summary

Motivation Neutrino Energy

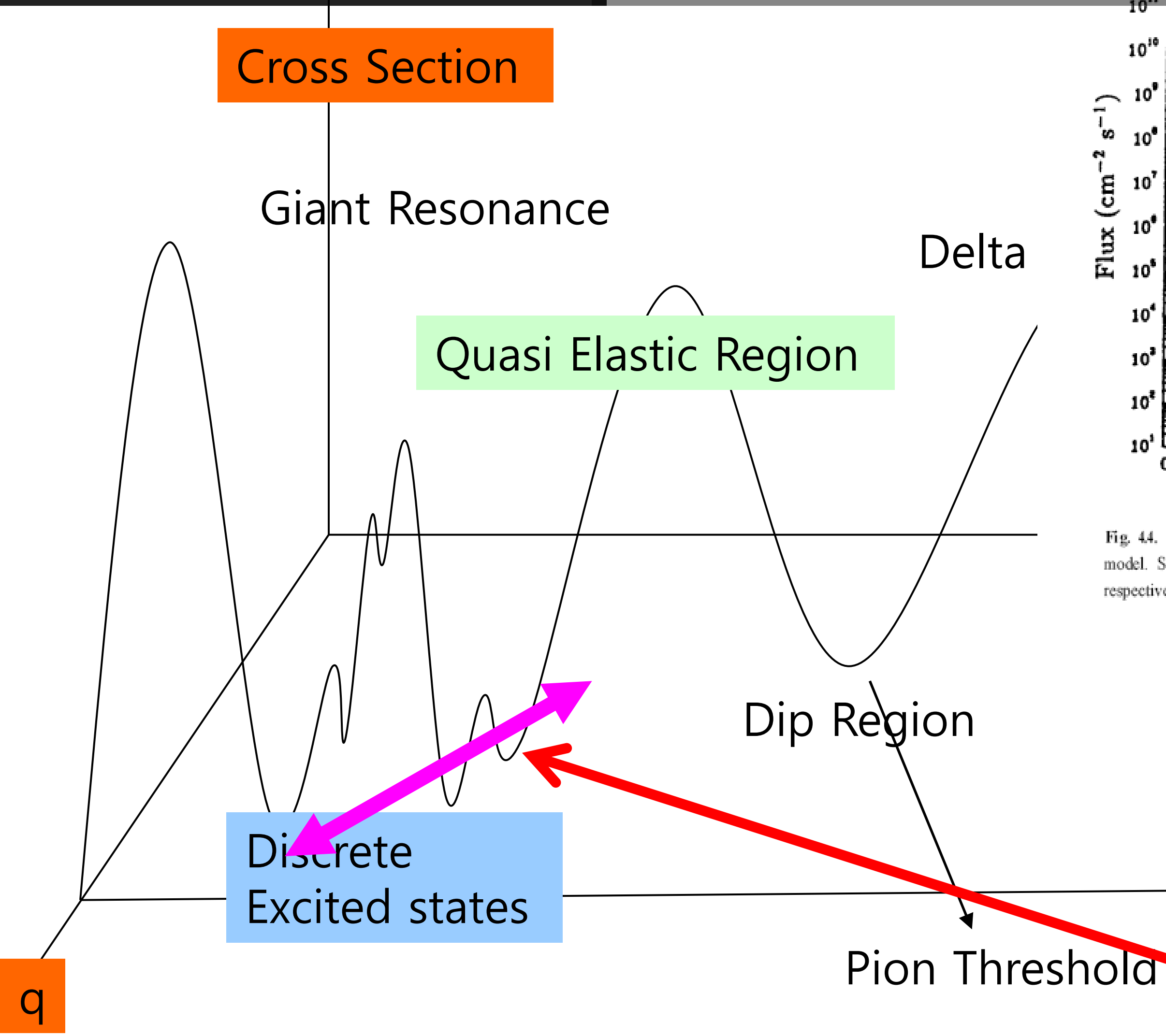

Typical cross section by incident electron

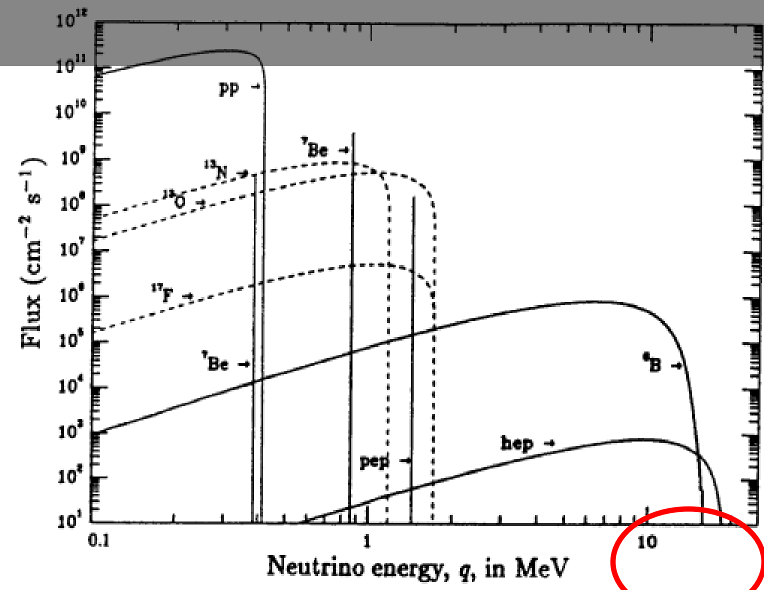

Fig. 44. Solar neutrino spectrum. Energy spectrum of solar neutrinos, as predicted by the standard solar model. Solid and dashed curves distinguish between neutrinos produced in the pp-chains and the CNO cycle, respectively. (From 49.)

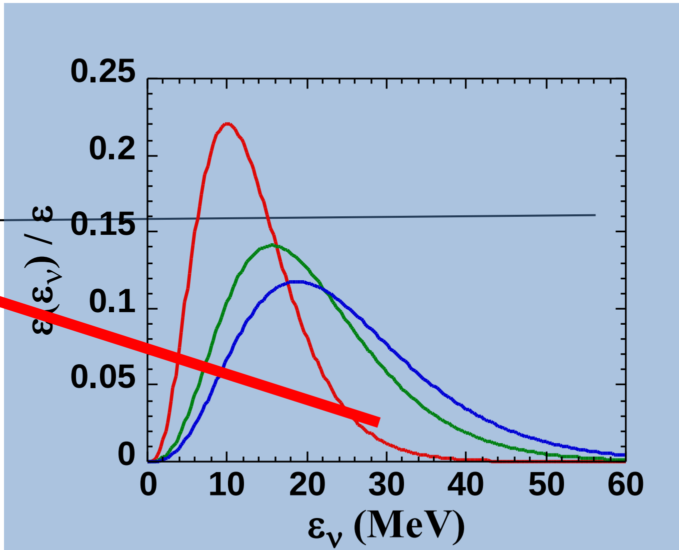

$T(\nu_e) = 3.2\ \mathrm{MeV} < T(\bar{\nu}_e) = 5.0\ \mathrm{MeV} < T(\nu_{\mu,\tau}) = T(\bar{\nu}_{\mu,\tau}) = 6.0\ \mathrm{MeV}$

FLOW of Computer Program (DQRPA)

1. Hartree Fock Field (Mean Field Potential)

Particle-Hole Interaction (Long Range)

Quasi -Particle (ph,pp,hh interactions) and Deformations

2. Deformed Bardeen Cooper Schriffer (DBCS) Theory

Pairing Correlations among different states

With G-matrix for NN interaction in nuclei

3. Hartree Fock Bogoliubob(HFB) Theory

Excited States

4. Deformed Quasi-particle RPA (DQRPA)

5. Beta Decay, Proton capture, Photo-disintegration….

6. Network Calculations for rp Nucleosynthesis

Cross Sections

$$\left(\frac{d\sigma_\nu}{d\Omega}\right)_{(\nu/\bar{\nu})} = \frac{G_F^2 \epsilon k}{\pi\ (2J_i+1)} \Big[\sum_{J=0} \cancelto{1}{(1+\vec{\nu}\cdot\vec{\beta})} | < J_f||\hat{\mathcal{M}}_J||J_i > |^2$$

$$+\cancelto{1}{(1-\vec{\nu}\cdot\vec{\beta}+2(\hat{\nu}\cdot\hat{q})(\hat{q}\cdot\vec{\beta}))} | < J_f||\hat{\mathcal{L}}_J||J_i > |^2 -$$

$$\cancelto{1}{\hat{q}\cdot(\hat{\nu}+\vec{\beta})} 2Re < J_f||\hat{\mathcal{L}}_J||J_i > < J_f||\hat{\mathcal{M}}_J||J_i >^*$$

$$+\sum_{J=1} \cancelto{1}{(1-(\hat{\nu}\cdot\hat{q})(\hat{q}\cdot\vec{\beta}))} (| < J_f||\hat{\mathcal{T}}_J^{el}||J_i > |^2 + | < J_f||\hat{\mathcal{T}}_J^{mag}||J_i > |^2)$$

$$\pm \sum_{J=1} \cancelto{-1}{\hat{q}\cdot(\hat{\nu}-\vec{\beta})} 2Re[< J_f||\hat{\mathcal{T}}_J^{mag}||J_i > < J_f||\hat{\mathcal{T}}_J^{el}||J_i >^*]\Big] ,$$

$$\sigma(E_\nu) = \frac{G_F^2 cos^2\theta_c}{\pi \hbar^4 c^3} \sum_i k_i \epsilon_i F(Z,\epsilon_i)[B_i(GT)+B_i(F)] , \qquad (8)$$

where k_i and ϵ_i refer to the momentum and total energy of the outgoing electron and $F(Z,\epsilon_i)$

$$R_T(\mathbf{q},\omega) = \Sigma_{J=0} | < J_f||\hat{\mathcal{T}}_J^{el}(\mathbf{q})||J_i > |^2 + | < J_f||\hat{\mathcal{T}}_J^{mag}(\mathbf{q})||J_i > |^2 ,$$

$$R_I(\mathbf{q},\omega) = \Sigma_{J=0} 2Re < J_f||\hat{\mathcal{T}}_J^{el}(\mathbf{q})||J_i > < J_f||\hat{\mathcal{T}}_J^{mag}(\mathbf{q})||J_i > ,$$

$$\left(\frac{d\sigma_\nu}{d\mathbf{q}^2}\right)^{ERL}_{\nu/\bar{\nu}} = \frac{2G_F^2 \epsilon cos^2(\frac{\theta}{2})}{\nu\ 2(J_i+1)} \left[R_{CL}(\mathbf{q},\omega) + C(\theta,\mathbf{q}) R_T(\mathbf{q},\omega) \mp tan(\frac{\theta}{2}) C(\theta,\mathbf{q}) R_I(\mathbf{q},\omega) \right]$$

Difference between two formalism for nu X-section

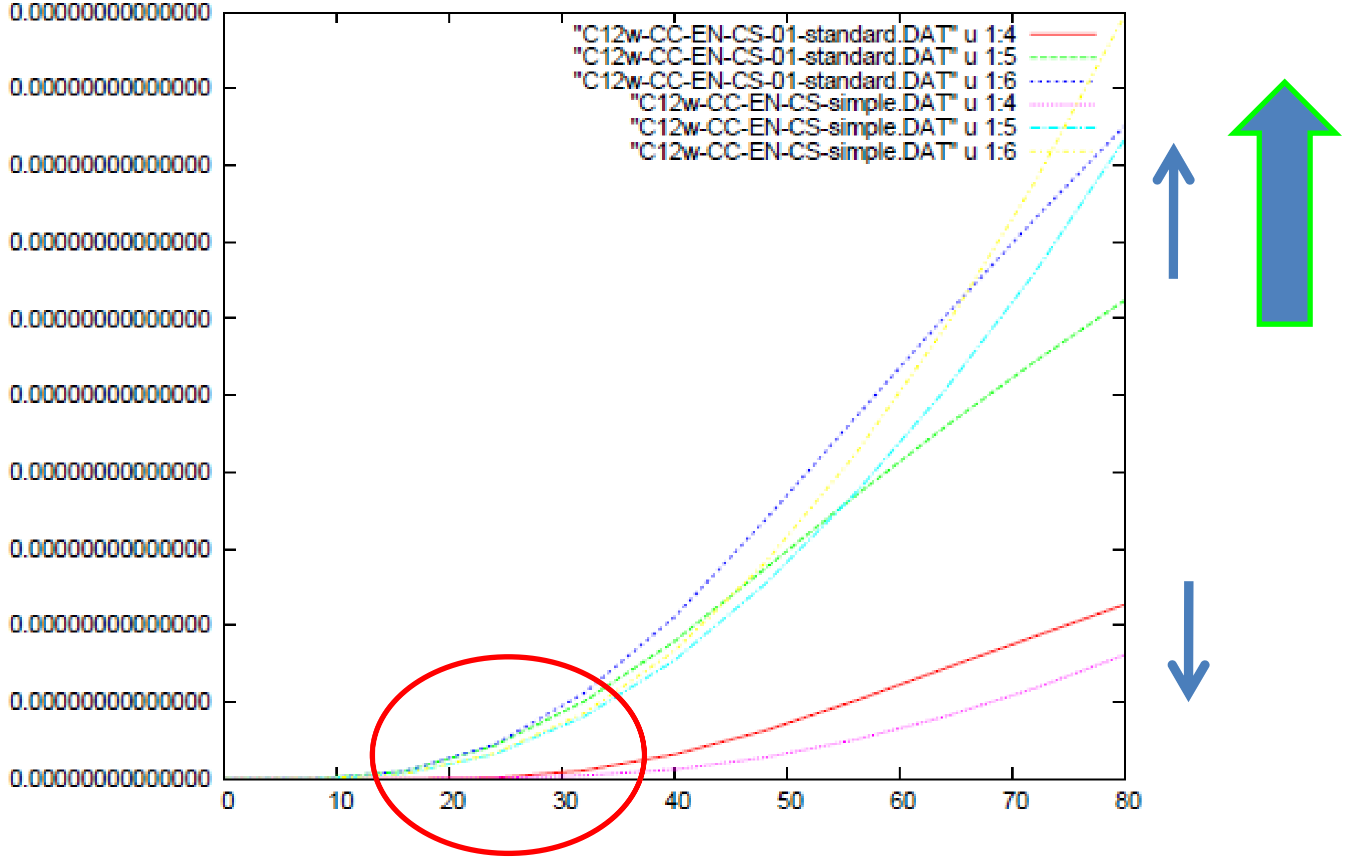

FIG. 8:

LSND : $\nu_e{}^{12}C \rightarrow e^- + {}^{12}N^*$

1 We need more data on nu reactions ! Neutrino beam from pion or

2. GT transitions by CEX are largely appreciated !
Roles of RIF for unstable nuclei are important for unstable nuclei !

3. Multi-pole transitions as well as GT should be considered !

4. Coulomb distortion beyond Fermi function for beta decay may work !

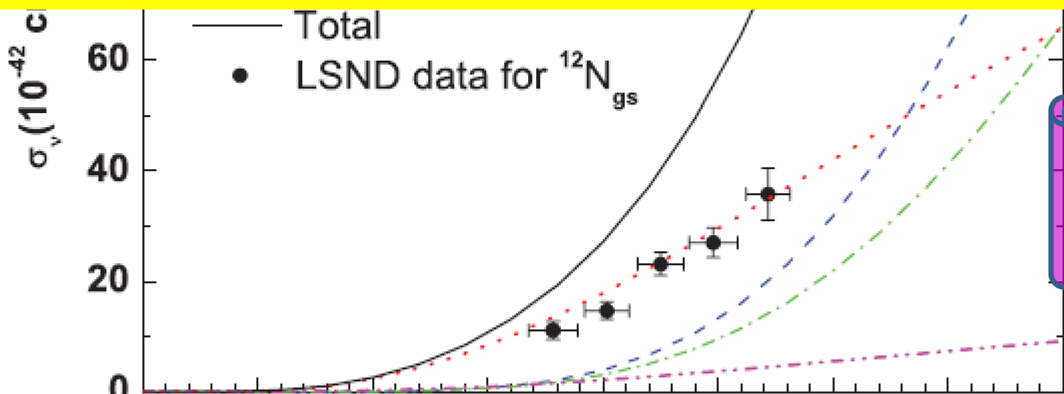

Cheoun, Ha, Lee, Kim, So, Kajino, PRC81, 028501(2010)

5. Contributions from higher energy tails,

6. How are effects from the bound nucleon in nuclei ?
Already discussed

7. How to treat the deformed nuclei ?

GT Results for 90Zr

Physics Letters B 615 (2005) 193–199
K. Yako [a], H. Sakai [a,b],

90Zr : beta- =6111KeV, beta+=2280 KeV

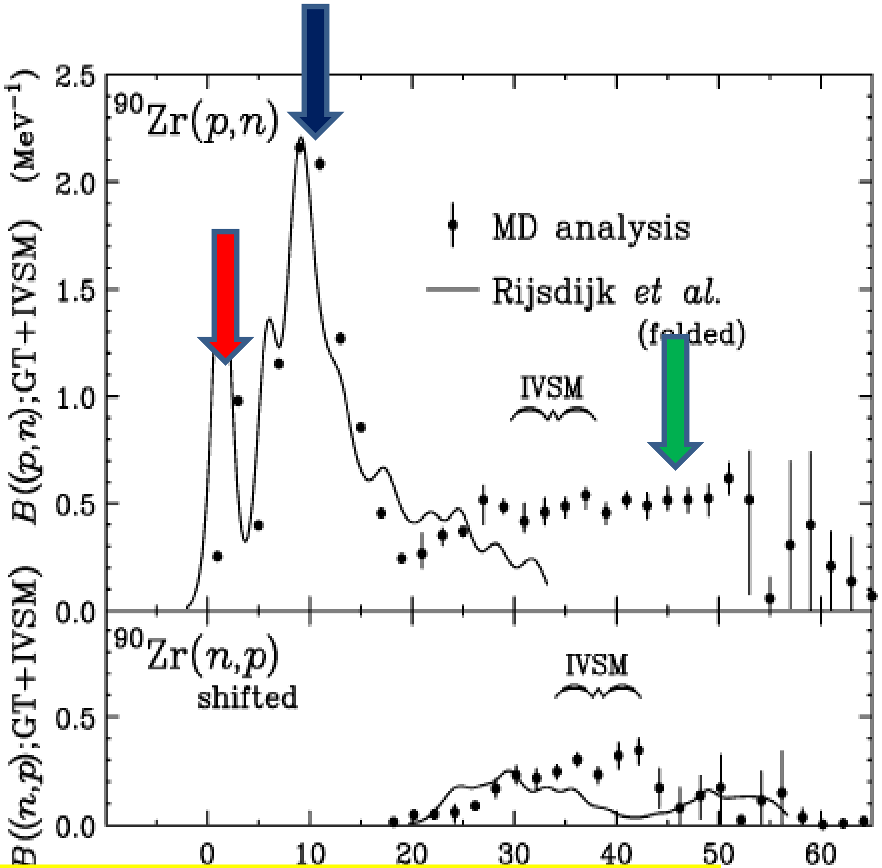

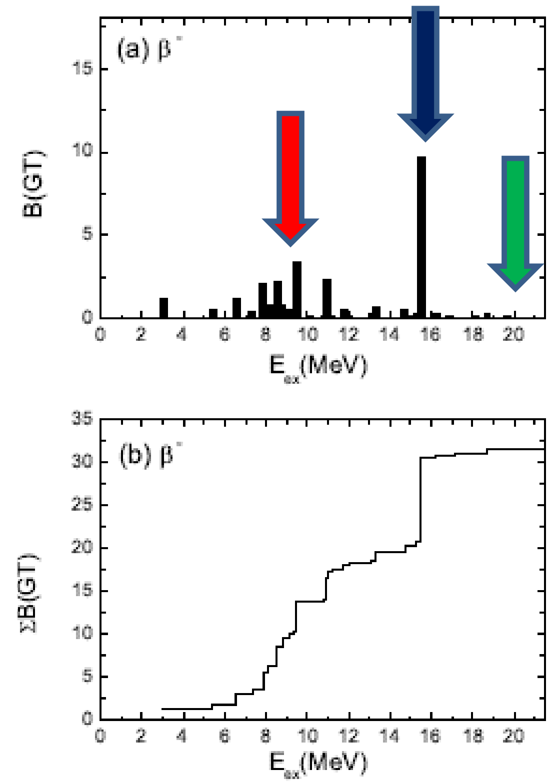

ISR is recovered
by high-lying GT excitation
coming from 2p-2h correlations.
Then, g_A quenching problem ??

states are well pointed.

gh-lying GT states.

ation energy

E_{ex} in the daughter nucleus ^{90}Cu. Left panel (Right) is without (with) np pairing correlations.

In spherical basis, J is a good quantum number.
But in deformed basis, a projection of J on the nuclear symmetric axis z, Ω, is a good quantum number.

Deformed states, $\pm 5/2$, $\pm 3/2$, and $\pm 1/2$, are separated from the spherical state $d_{5/2}$.

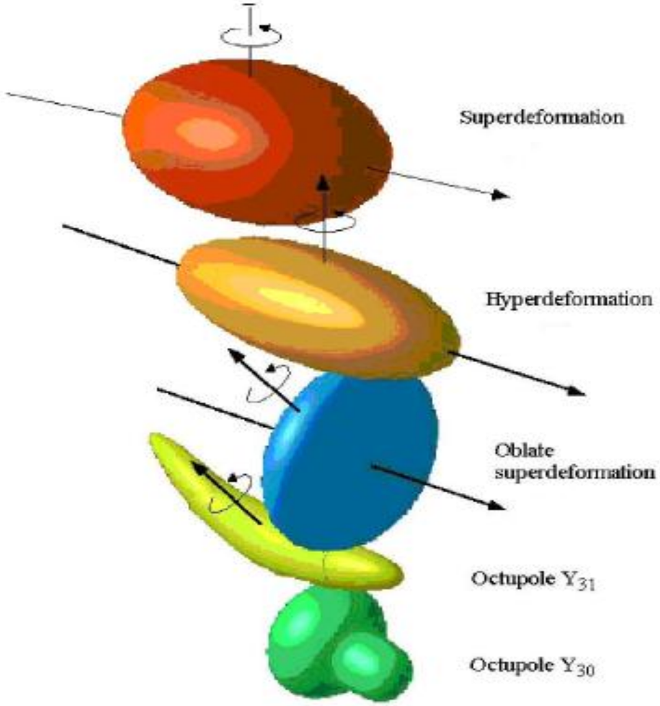

Figure 1.2. Various shapes observed or expected in nuclei. Exotic orbitals that appear in regions far from the stability line may provide some new types of deformation. The superdeformation (top) and pear shape (bottom) have been observed experimentally; the oblate superdeformation has been predicted but not observed—less deformed oblate shapes are, however, quite common. The hyperdeformation (second from the top) has been seen in certain nuclei. The octupole banana-type deformation has not been observed in such extreme form, but vibrations of this kind are well known.

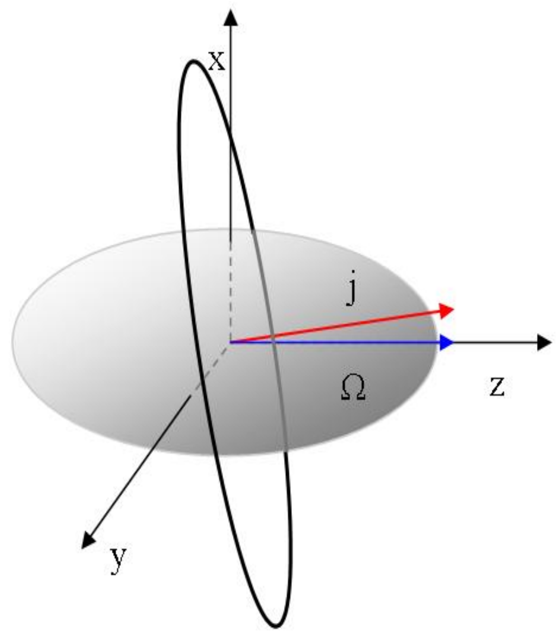

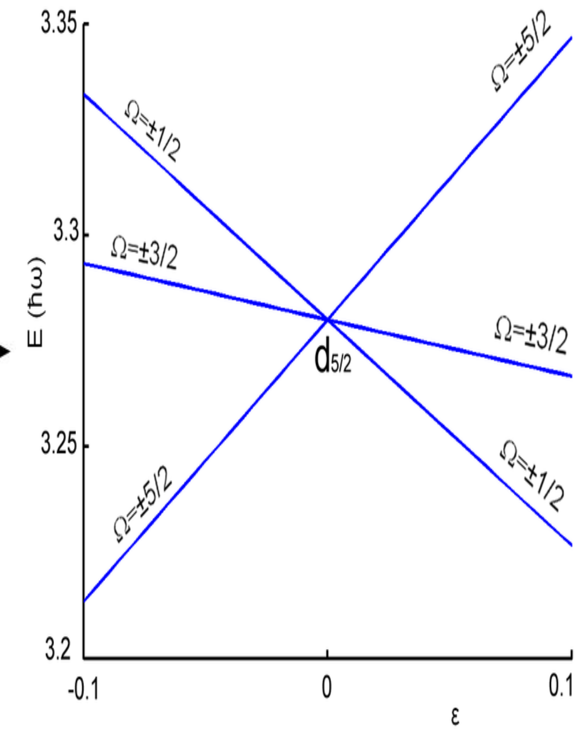

➢ Single particle states in deformed nucleus become more complex.

Deformed QRPA From spherical basis to Nilsson basis

$$|\alpha\Omega_\alpha > = \sum B^\alpha_a |a\Omega_\alpha > \qquad B^\alpha_a = \sum_{N n_z \Sigma} C^{j\Omega_\alpha}_{l\Lambda\frac{1}{2}\Sigma} A^{n_r l}_{N n_z \Lambda}\, b_{N n_z \Sigma}. \quad A^{n_r l}_{N n_z \Lambda} =< n_r l \Lambda | N n_z \Lambda >$$

$$|\alpha\bar{\beta} > = \sum_{abJ} F^{JK}_{\alpha a} |ab,\ JK > = \sum_J C^{JK}_{j_a\Omega_a j_b\Omega_b} |a\Omega_a > |b\Omega_b >, \text{ and } F^{JK}_{\alpha a\beta b} = B^\alpha_a\, B^\beta_b (-1)^{j_\beta-\Omega_\beta}\, C^{JK}_{j_a\Omega_a j_\beta-\Omega_\beta}$$

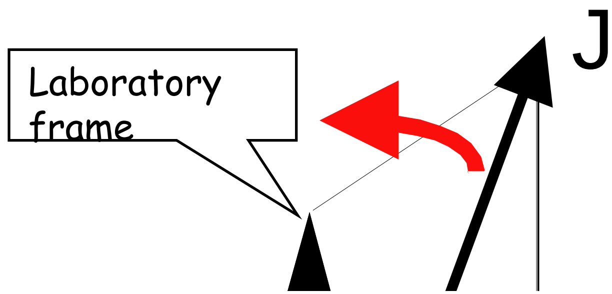

Normal-parity orbits;

| [411 3/2] > = 0.926 | 411 3/2> + …
= 0.418 $|g_{9/2}>$ – 0.140 $|g_{7/2}>$ + 0.864 $|d_{5/2}>$ + 0.246 $|d_{3/2}>$

| [411 1/2] > = 0.900 | 411 1/2> + …
= – 0.163 $|g_{9/2}>$ + 0.396 $|g_{7/2}>$ – 0.099 $|d_{5/2}>$ + 0.848 $|d_{3/2}>$ + 0.297$|s_{1/2}>$

| [400 1/2] > = 0.968 | 400 1/2> + …
= 0.147 $|g_{9/2}>$ – 0.072 $|g_{7/2}>$ + 0.539 $|d_{5/2}>$ – 0.160 $|d_{3/2}>$ + 0.811 $|s_{1/2}>$

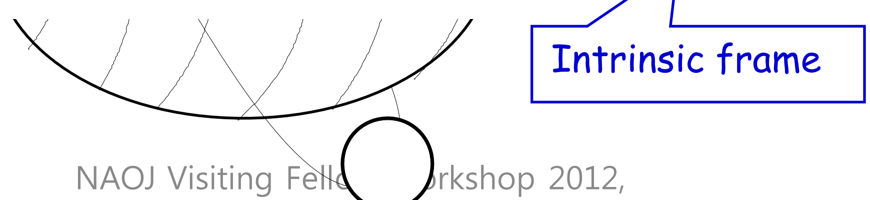

Result 1

Gamow-Teller Strengths on $^{26-34}$Mg isotopes by the Deformed Quasi-particle RPA

Shell Evolution by the deformation

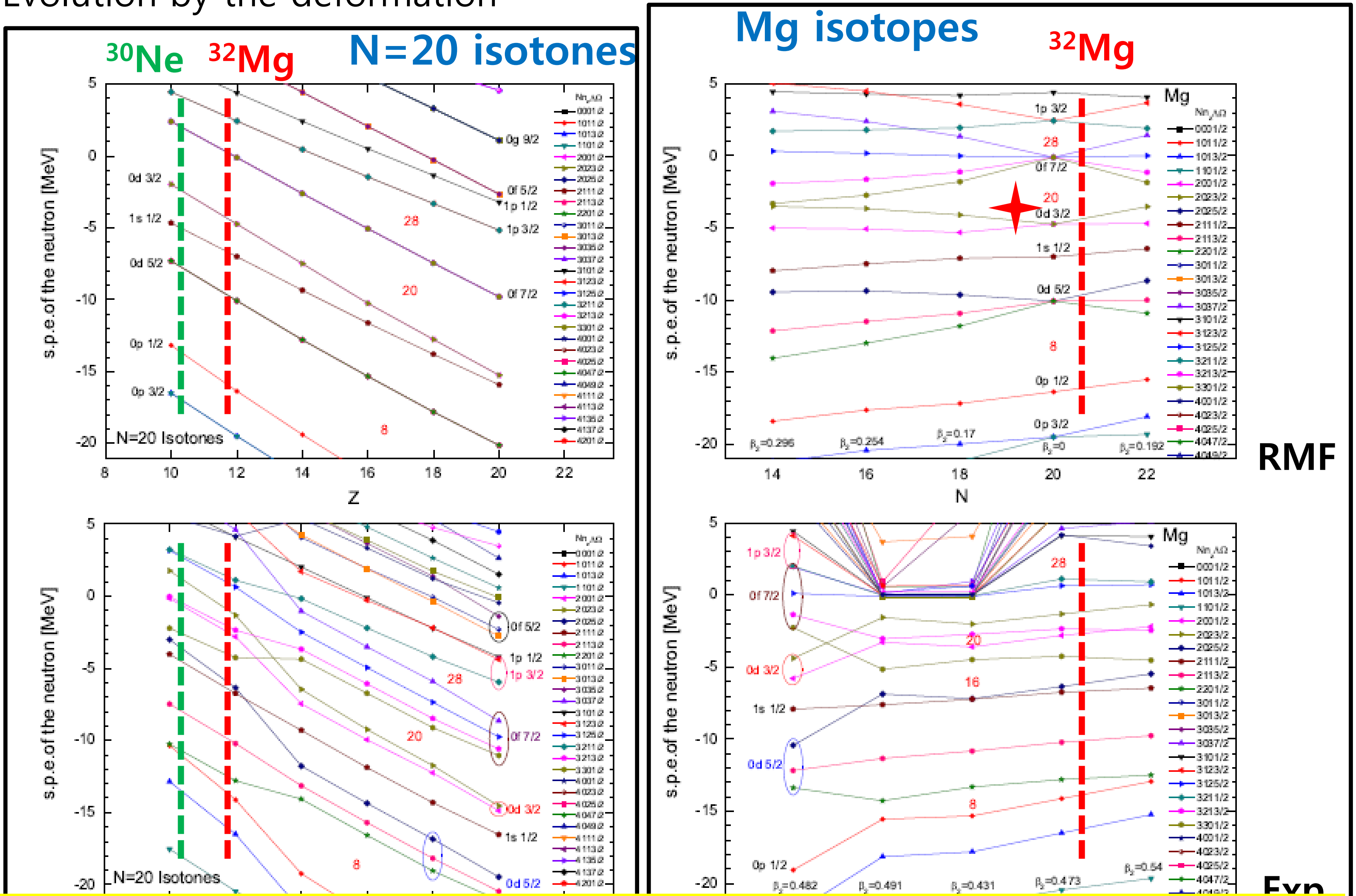

1. N = 20 magic number disappeared in ^{32} Mg. But N = 28 is still the

2. ^{30}Ne shows degeneracy of fp shells .

Deformed QRPA GT strength distributions on 26 Mg

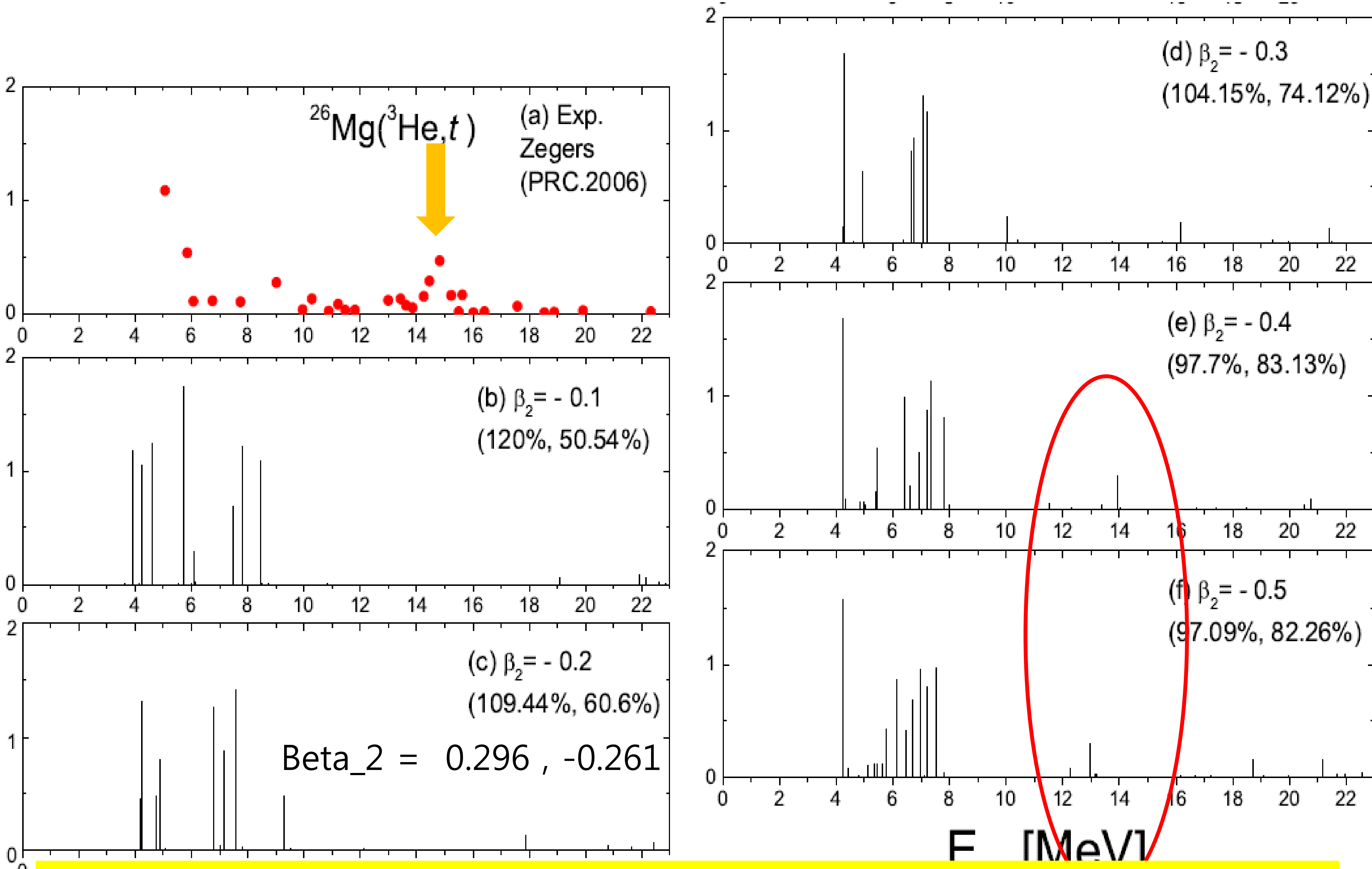

Oblate deformation leads to high lying GT states. ! Nothing in prolate.

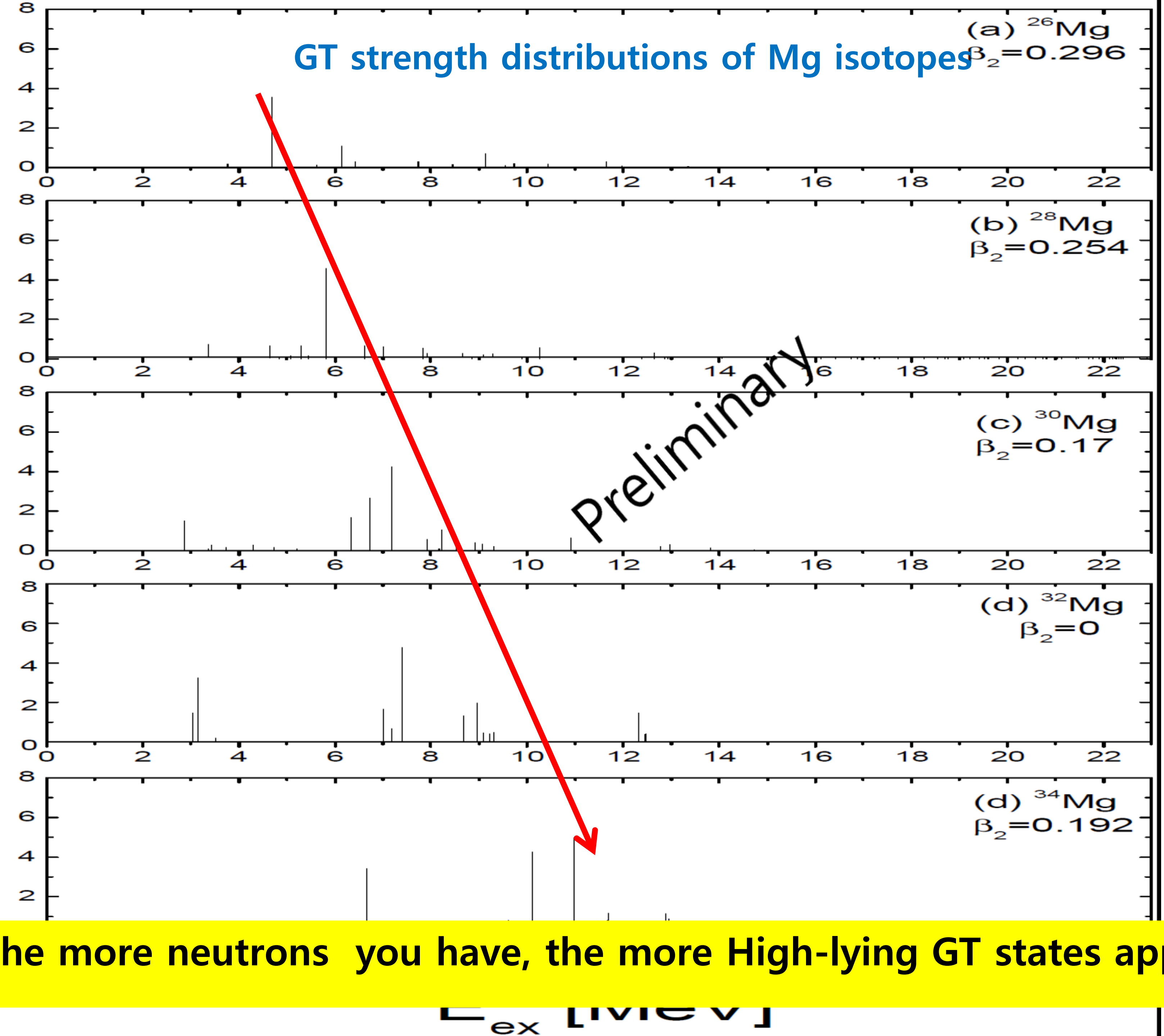

The more neutrons you have, the more High-lying GT states appear.

Neutrino X-section on deformed 26 Mg which show a change about tens of % compared to the result by small deformation

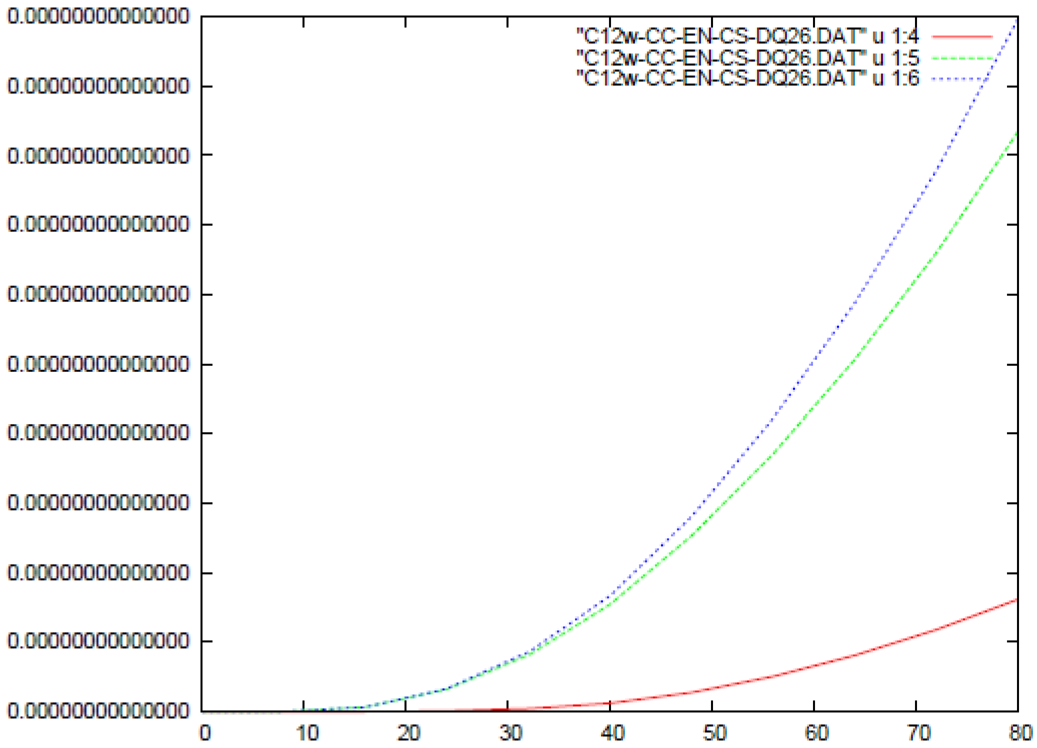

FIG. 9:

Result 3

High-lying Gamow-Teller excited states in the deformed nuclei of ^{76}Ge and ^{82}Se by the Deformed Quasi-particle RPA

arXiv : 1206.2156[nucl-th] (2012)

❖ Calculated GT states on ^{76}Ge and ^{82}Se.

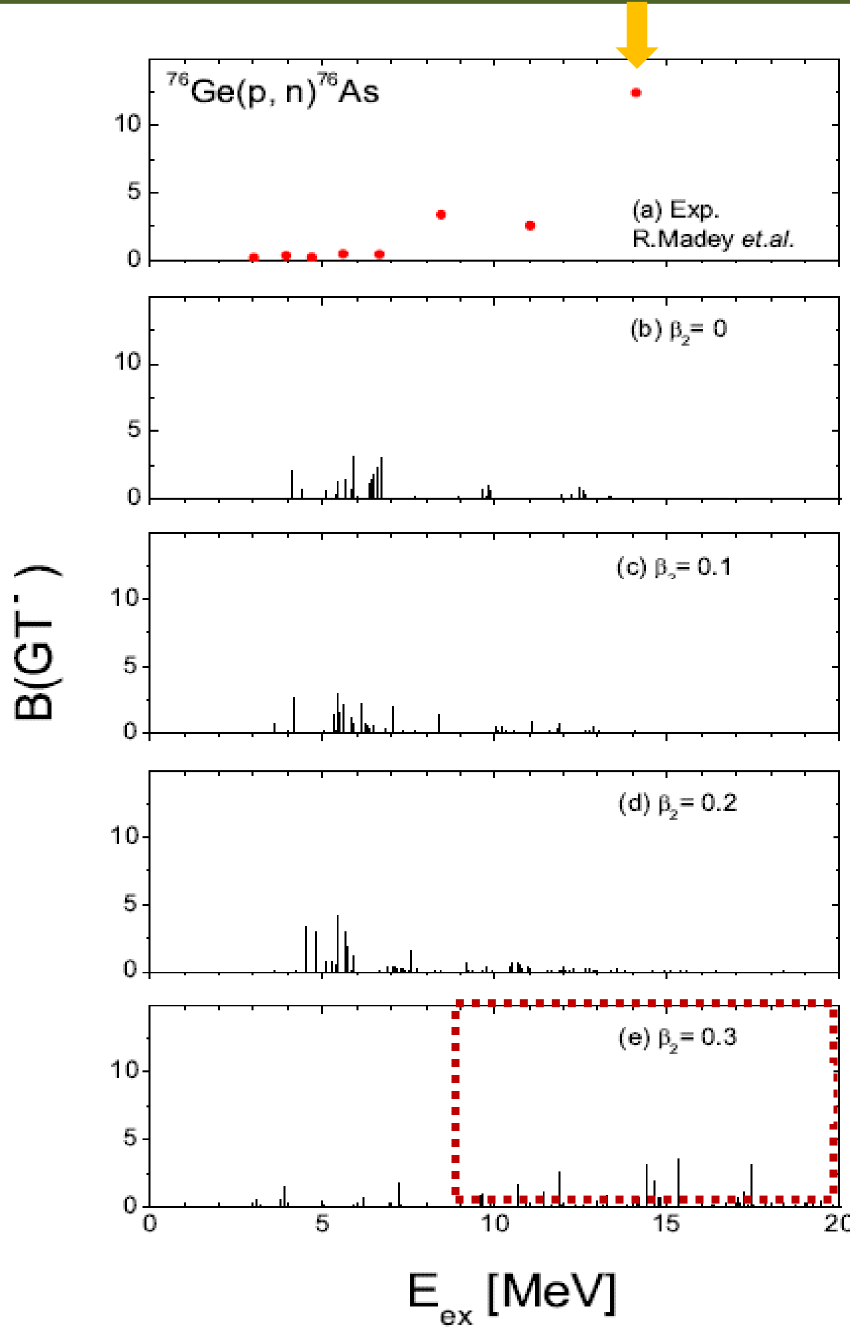

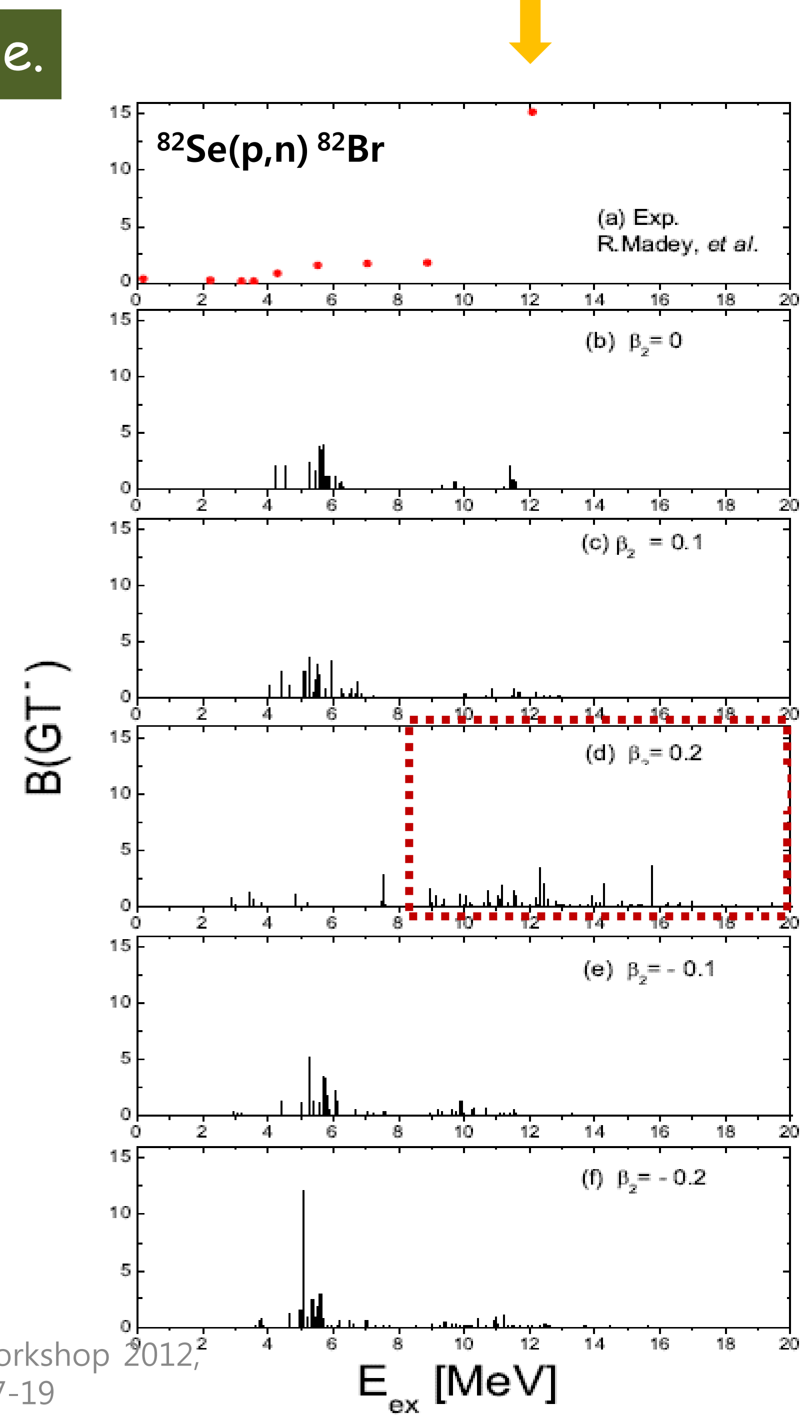

/orkshop 2012,
.7-19

Deformed QRPA GT strength distributions on 76 Ge and 82 Se

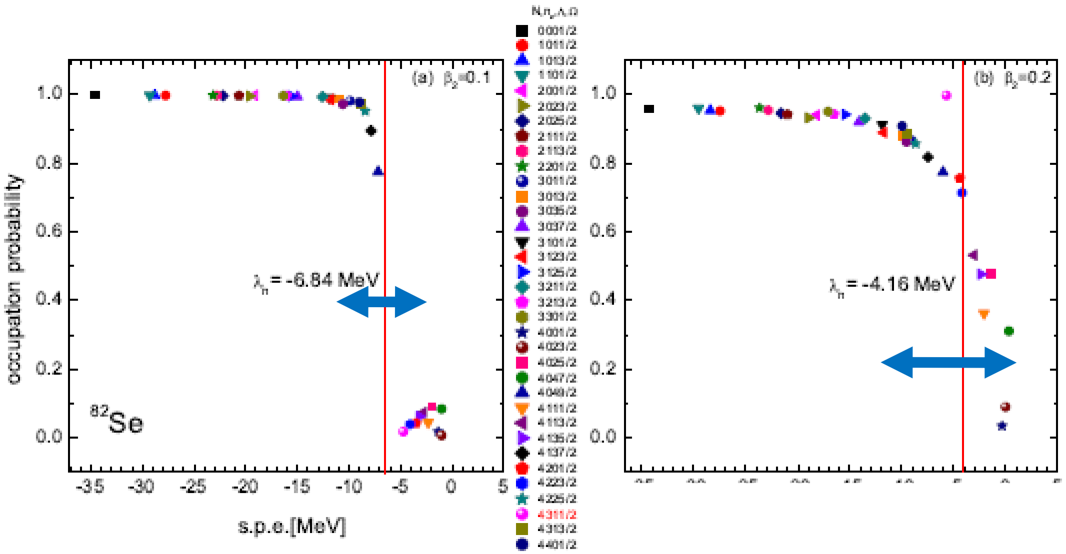

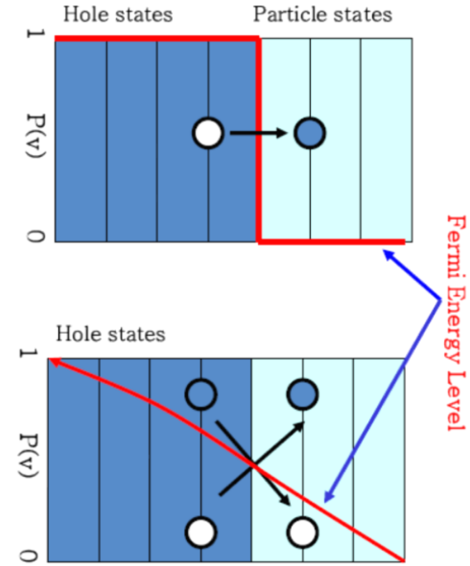

FIG. 1: (Color online) Occupation probability of the neutron of ^{82}Se with two deformation parameters β_2 as a function of the single particle energy given as Nilsson basis.

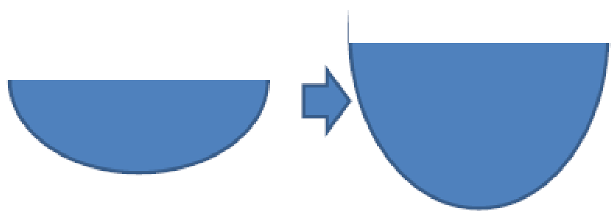

Deformation ->

Fermi energy increase ->

Wide Fermi smearing ->

2p-2h mixing ->

High-lying excitations are intimately associated with the deformation !!

excitation

The first University in Korea
Soongsil University

Summary

1. More data are necessary for understanding neutrino-induced reactions.
   DIF of pions or Beta beam neutrinos from RI are plausible sources of neutrinos on the lab. on Earth.
2. GT transitions are welcome because they dominate low energy X-section.
   In specific, RIB Facilities may greatly contribute to the CEX on the unstable nuclei.
3. Multi-pole transitions as well as GT should be considered !
4. Coulomb distortion beyond Fermi function for beta decay may work !
5. Contributions from higher energy tails, high-lying excited states beyond 1 nucleon threshold , also contribute .
   More CEX data beyond 1 nucleon threshold are necessary.
6. To treat density dependence is also necessary.
7. DQRPA is a quite useful for the nu-reaction description of deformed nuclei

Thanks for your attention,
and
NAOJ
for this workshop !